UCRL-JRNL-214778

LAWRENCE
LIVERMORE
NATIONAL
LABORATORY

Coupled Climate Model Appraisal a Benchmark for Future Studies

T. J. Phillips, K. AchutaRao, D. Bader, C. Covey, C. M. Doutriaux, M. Fiorino, P. J. Gleckler, K. R. Sperber, K. E. Taylor

August 23, 2005

Eos

Disclaimer

UCRL-JRNL-214778

Coupled Climate Model Appraisal a Benchmark for Future Studies

Thomas J. Phillips, Krishna AchutaRao, David Bader, Curtis Covey, Charles M. Doutriaux, Michael Fiorino, Peter J. Gleckler, Kenneth R. Sperber, and Karl E. Taylor

Program for Climate Model Diagnosis and Intercomparison (PCMDI)
Lawrence Livermore National Laboratory
Livermore, California 94551

Submitted to *Eos*
August 24, 2005

Corresponding author's address:
Thomas J. Phillips
Lawrence Livermore National Laboratory, Mail Code L-103
P.O. Box 808
Livermore, California 94551
Phone: 925-422-0072
Fax: 925-422-7675
e-mail: phillips14@llnl.gov

The Program for Climate Model Diagnosis and Intercomparison (PCMDI) has produced an extensive appraisal of simulations of present-day climate by eleven representative coupled ocean-atmosphere general circulation models (OAGCMs) which were developed during the period 1995-2002 (PCMDI 2004, http://www-pcmdi.llnl.gov/model_ appraisal.pdf). Because projections of potential future global climate change are derived chiefly from OAGCMs, there is a continuing need to test the credibility of these predictions by evaluating model performance in simulating the historically observed climate. For example, such an evaluation is an integral part of the periodic assessments of climate change that are reported by the Intergovernmental Panel on Climate Change (IPCC, http://www.ipcc.ch/). The PCMDI appraisal thus provides a useful benchmark for future studies of this type.

The appraisal mainly analyzed multi-decadal simulations of present-day climate by models that employed diverse representations of climate processes for atmosphere, ocean, sea ice, and land, as well as different techniques for coupling these components (see Table). The selected models were a subset of those entered in phase 2 of the Coupled Model Intercomparison Project (CMIP2, Covey et al. 2003). For these "CMIP2+ models", more atmospheric or oceanic variables were provided than the minimum requirements for participation in CMIP2. However, the appraisal only considered those climate variables that were supplied from most of the CMIP2+ models.

The appraisal focused on three facets of the simulations of current global climate: 1) secular trends in simulation time series which would be indicative of a problematical "coupled climate drift"; 2) comparisons of temporally averaged fields of simulated atmospheric and oceanic climate variables with available observational climatologies;

and 3) correspondences between simulated and observed modes of climatic variability. Highlights of these climatic aspects manifested by different CMIP2+ simulations are briefly discussed here.

Secular Trends

To identify instances of coupled climate drift, the magnitudes of secular trends in the simulations of surface air and ocean temperatures, in total sea ice extents, and in deep ocean temperatures and salinities were examined. No substantial drift in any simulation of surface temperature was found. Trends in global average sea surface temperatures (SSTs), for example, were generally less than 0.4 K/century in absolute magnitude, even for the three models (CCSM2, HadCM3, and PCM) that did not apply surface flux adjustments to ameliorate coupled climate drift (Sausen et al. 1988).

Although larger trends were present in deep ocean temperatures and salinities and in total sea ice extents, these were small enough to confirm that each coupled model had achieved a quasi-equilibrated climate state (Covey et al. 2005). The absence of substantial large-scale trends also implied that time-mean climatologies of atmospheric and oceanic variables derived from the simulations were representative of the models' coupled climate states.

Climatologies

The collective performance of the coupled models in simulating the observed mean climate, as indicated by 20-year climatologies of diverse atmospheric and oceanic variables, also was evaluated. The atmospheric analysis focused on features of the mean of the ensemble of different model values at each point of a climatic field after remapping to a common (~3x3-degree) grid. Because this multi-model ensemble-mean climatology usually agreed better with corresponding global atmospheric observations than any single simulation (owing to a partial cancellation of individual model errors from the ensemble averaging), deviations of this ensemble mean from the observational climatology were indicative of general problems in the CMIP2+ models.

For instance, comparisons of seasonal climatologies of ensemble-mean model precipitation with corresponding observational estimates (Figure 1) showed similarities in large-scale patterns, but the simulated precipitation amounts were excessive in the subtropical eastern oceans and were deficient in the tropical convergence zones, especially in the June-July-August (JJA) season. (These discrepancies were consistent with generally low values of tropical atmospheric humidity in most of the models--not shown here.) Inter-model variations in precipitation (bottom row of Figure 1) were also large in the tropical convergence zones, and to a lesser extent in the mid-latitude storm tracks, indicating substantial differences in the individual simulations of such finer-scale phenomena.

Each model's combination of annual-mean precipitation and surface air temperature also was categorized regionally according to the geographically based Köppen classification scheme. The typical model's rendering of the five major Köppen climatic regimes (tropical, desert/steppe, temperate, snowy, and polar) compared well with observational estimates over most of the continental surfaces, and the agreement was better still for the ensemble-mean model climatology (Fiorino 2005).

In addition, goodness-of-fit measures were calculated between many different multi-model ensemble-mean atmospheric climatological fields and the corresponding observational estimates (Taylor 2001). The best agreement with available observations was found in simulated mid-tropospheric geopotential height, lower-tropospheric humidity, mean sea-level pressure, top-of-atmosphere (TOA) outgoing longwave radiation, surface air temperature, and upper-tropospheric winds. Intermediate degrees of similarity were displayed by fields of TOA upward shortwave radiative fluxes and longwave cloud radiative forcing, surface wind stresses, and precipitation. The poorest agreements with observations were found in simulated surface sensible and latent heat fluxes, total cloud cover, and especially in upper-tropospheric temperatures—a persistent problem in many global climate models.

The appraisal of simulated ocean variables compared 20-year climatological profiles of temperature and salinity in each model with available observational estimates (Levitus and Boyer 1994, Levitus et al. 1994) for the major ocean basins. Because some variant of the Levitus estimates had been used to initialize the ocean components of all the models prior to their coupled spin-up (see Table), continued qualitative similarities of the simulated deep-ocean temperatures and salinities with the Levitus data were anticipated. This expectation was mostly confirmed, except in the Arctic Ocean where the generally poor model comparisons with Levitus estimates may be attributable to shortcomings in simulating oceanic vertical mixing, inter-basin heat/salinity exchanges, or the insulating effects of sea ice.

Model upper-ocean variables also differed somewhat from the Levitus data, as seen for example in cross sections of simulated equatorial Pacific upper-ocean temperatures (Figure 2). While all the models displayed the correct sign of the east-west equatorial temperature gradient (warm West Pacific and cold East Pacific), they showed mixed success in replicating the Levitus estimates of the steepness of this ocean temperature gradient and of max/min temperatures.

Simulation differences in tropical north-south ocean temperature gradients also resulted in sizeable deviations of model equatorial Pacific currents from observationally based analyses, with some coupled models producing an anomalous equatorial South Pacific counter-current (not shown). In other basins, where observational estimates were not available, ocean currents simulated by different models displayed qualitative similarities, but substantial intensity variations.

Climatic Variability

Recurring modes of variability about the mean atmospheric climatologies over a range of frequencies also were analyzed. These modes included synoptic tropical waves and the intra-seasonal Madden-Julian Oscillation (MJO), as well as the lower-frequency North Atlantic Oscillation (NAO) and El Niño/Southern Oscillation (ENSO).

In the case of the ENSO, for instance, some models performed markedly better than others (Figure 3). Most models showed a seasonal phase-locking of their composite warm ENSO events, with maximum amplitude occurring in Northern winter in agreement with observations (Figure 3a). However, the amplitudes of some modeled ENSOs fell outside the one-standard-deviation envelope of the observed warm events, with several simulations being much too weak, and a few too strong. The overly weak events failed to reproduce the observed periodicity of 2 to 7 years (Figure 3b), while the peak power of the overly strong events occurred mostly at the lower end of this range.

A more detailed comparison (not shown) of the warm-event characteristics with those of antecedent model simulations analyzed by AchutaRao and Sperber (2002) implied that the more recently developed CMIP2+ models tended to simulate the ENSO mode with greater realism. Current-vintage OAGCMs generally show even more improvement (AchutaRao and Sperber 2005).

Future Studies

While the PCMDI appraisal is more extensive than previous analyses of this type, it renders only a performance "snapshot" of coupled climate models which are undergoing continual development. The appraisal's enduring value is that it provides a benchmark against which to measure the performance of current-vintage coupled climate models.

Especially noteworthy for future studies of this type are the multiple simulations of historical climate and potential future climate change which recently have been produced by some two dozen OAGCMs in support of the IPCC's Fourth Assessment Report, which is scheduled for publication in 2007. These simulations comprise substantially more comprehensive model output data than were previously available, and thus will require unprecedented cooperative efforts to thoroughly analyze.

To this end, PCMDI is providing storage facilities and associated infrastructural support for efficiently disseminating these model data to the scores of climate scientists who are contributing to this formidable task (http://www-pcmdi.llnl.gov/ipcc/about_ipcc.php). In addition, PCMDI plans to extend and update its coupled model appraisal to reflect the wealth of new data provided by the IPCC simulations. This commitment also demands the continuing enhancement and refinement of PCMDI's working set of diagnostic methods, data-management tools, and visualization and computation software (http://www-pcmdi.llnl.gov/software/about_software.php), and their broad distribution within the international climate community.

Acknowledgments

We are grateful to the participating model sponsors* for making available supplemental output data for the PCMDI appraisal. The work of PCMDI is supported by the U.S. Department of Energy, Office of Science, Climate Change Prediction Program and is performed at the University of California Lawrence Livermore National Laboratory under Contract W-7405-Eng-48.

*Canadian Centre for Climate Modelling and Analysis (CCCma), Victoria, Canada; Commonwealth Scientific and Industrial Research Organization (CSIRO), Mordialloc, Australia; U.S. Department of Energy (DOE), Gaithersburg, Maryland; Geophysical Fluid Dynamics Laboratory (GFDL), Princeton, New Jersey; Max Planck Institute for Meteorology (MPI), Hamburg, Germany; Meteorological Office (MO), Exeter, United Kingdom; Meteorological Research Institute (MRI), Ibaraki, Japan; Model & Data Group (M&D), Hamburg, Germany; National Center for Atmospheric Research (NCAR), Boulder, Colorado; and University of Bergen (UB), Bergen, Norway.

References

AchutaRao, K. and K. R. Sperber, 2002: Simulation of the El Niño Southern Oscillation: Results from the coupled model intercomparison project. *Climate Dyn*., **19**, 191-209.

AchutaRao, K. and K. R. Sperber, 2005: ENSO simulation in coupled ocean-atmosphere models: Are the current models better? *Climate Dyn.* (submitted).

Covey, C., K.M. AchutaRao, U. Cubasch, P. Jones, S.J. Lambert, M.E. Mann, T.J. Phillips and K.E. Taylor, 2003: An overview of results from the Coupled Model Intercomparison Project, *Glob. Planet. Change*, **37**, 103-133.

Covey, C., P.J. Gleckler, T.J. Phillips, and D. Bader, 2005: Secular trends and climate drift in coupled ocean-atmosphere general circulation models. *J. Geophys. Res.*. (submitted).

Fiorino, M., 2005: An assessment of climate model performance using the Köppen classification system. *Climate Dyn.* (submitted).

Levitus, S. and T.P. Boyer, 1994: World ocean atlas 1994, Vol. 4: Temperature. NOAA/NESDIS E/OC21, U.S. Department of Commerce, Washington, D.C., 117 pp.

Levitus, S., R. Burgett, and T.P. Boyer 1994: World ocean atlas 1994, Vol. 3: Salinity. NOAA/NESDIS E/OC21, U.S. Department of Commerce, Washington, D.C., 99 pp.

PCMDI, 2004: An Appraisal of Coupled Climate Model Simulations. Editor: D. Bader, contributing authors: K. Achutarao, C. Covey, C. Doutriaux, M. Fiorino, P. Gleckler, T. Phillips, K. Sperber, and K. Taylor. Report UCRL-TR-202550, Program for Climate Model Diagnosis and Intercomparison, Lawrence Livermore National Laboratory, Livermore, California, 183 pp. Accessible online at http://www-pcmdi.llnl.gov/model_ appraisal.pdf.

Sausen, R., K. Barthels, and K. Hasselmann, 1988: Coupled ocean-atmosphere models with flux correction. *Climate Dyn.*, **2**, 145-163.

Taylor, K.E., 2001: Summarizing multiple aspects of model performance in a single diagram. *J. Geophys. Res.,* **106**, 7183-7192.

Table 1: Salient features of the CMIP2+ models and respective simulations of the present climate are listed. Among the included features are the approximate year of model development ("vintage"), and the institutional sponsor and country. Also listed are the horizontal and vertical resolution of the model atmosphere and ocean (approximate latitude x longitude size of a grid cell and the number of vertical levels L) as well as the pressure of the atmospheric top (in units of hecto-Pascals--hPa) and the vertical coordinate (depth or density) of the model ocean. The representation of sea ice dynamics and structure (explicit rheology, inclusion of ice leads), and of land hydrology (single-layer "bucket" or layered soil column) and vegetation (inclusion of canopy biophysics) also are indicated. In addition, selected aspects of the ocean-atmosphere coupling are noted, including the duration of the coupled spin-up prior to the nominal start of each simulation and the application of surface flux adjustments (in heat, freshwater, or momentum) designed to ameliorate model tendencies for "coupled climate drift".

Model, Vintage	**Institutional Sponsor, Country**	**Atmosphere:** Resolution Top Pressure	**Ocean:** Resolution Vertical coord.	**Sea Ice:** Dynamics Structure	**Land:** Soil Plants	**Coupling:** Coupled spin-up duration Surface flux adjustments
BCM02,2002	University of Bergen, Norway	1.9°×1.9° L31 10 hPa	2.4°×2.4° L24 density	rheology leads	layers canopy	25 years heat, freshwater
CCCma_CGCM2,2002	Canadian Centre for Climate Modelling & Analysis, Canada	3.7°×3.7°L10 5 hPa	1.9°×1.9° L29 depth	rheology leads	bucket no canopy	50 years heat, freshwater
CCSM2.0, 2002	National Center for Atmospheric Research, USA	2.8°×2.8°L26 2.9 hPa	1.0°×1.0° L40 depth	rheology leads	layers canopy	350 years no adjustments
CSIRO_Mk2,1997	Commonwealth Scientific & Industrial Research Organization, Australia	3.2°×5.6° L9 21 hPa	3.2°×5.6° L21 depth	rheology leads	layers canopy	105 years heat, freshwater, momentum
ECHAM4_OPYC3, 1996	Max Planck Institute for Meteorology, Germany	2.8°×2.8° L19 10 hPa	2.8°×2.8° L11 density	rheology leads	bucket canopy	100 years heat, freshwater
ECHO-G, 1999	Model & Data Group, Germany	3.8°×3.8° L19 10 hPa	3.8°×3.8° L20 depth	rheology leads	bucket canopy	310 years heat, freshwater anomalies
GFDL_R30_c, 1996	Geophysical Fluid Dynamics Laboratory, USA	2.3°×3.8° L14 15 hPa	1.9°×2.3° L18 depth	no rheology no leads	bucket no canopy	900 years heat, freshwater
HadCM2, 1995	Meteorological Office,UK	2.5°×3.8° L19 5 hPa	2.5°×3.8° L20 depth	no rheology leads	layers canopy	~ 500 years heat, freshwater
HadCM3, 1997		2.5°×3.8° L19 5 hPa	1.5°×1.5° L20 depth	no rheology leads	layers canopy	400 years no adjustments
MRI_CGCM2.3, 2002	Meteorological Research Institute, Japan	2.8°×2.8° L30 0.4 hPa	2.0°×2.5° L23 depth	no rheology leads	layers canopy	95 years heat, freshwater
PCM, 1999	Department of Energy, USA	2.8°×2.8° L18 2.9 hPa	0.7°×0.7° L32 depth	rheology leads	layers canopy	50 years no adjustments

Figure Captions

Figure 1. Simulation-observation comparisons of December-January-February (DJF) and June-July-August (JJA) total precipitation (in mm day^{-1}). First row: CPC Merged Analysis of Precipitation (CMAP) observation-based data (http://www.cdc.noaa.gov/cdc/data.cmap.html); second row: multi-model ensemble mean (BCM02 model data not included); third row: multi-model ensemble-mean departures from CMAP; bottom row: ensemble cross-model standard deviation. Note that nonlinear scales are used for all plots and that the multi-model ensemble statistics and observational estimates are interpolated to a common (~3 x 3-degree) grid.

Figure 2. Equatorial Pacific (averaged 2 S-2 N) simulations of 20-year climatologies of upper-ocean temperature in CMIP2+ models (ECHAM4-OPYC and HadCM2 models not included) compared with the estimates of Levitus and Boyer (1994).

Figure Captions, Continued

Figure 3: Aspects of CMIP2+ model simulations of the ENSO compared with observation-based estimates. In Figure 3a the evolution of the surface air temperature anomaly in the NIÑO3 region (5°S–5°N and 150°W–90°W) is shown for a composite warm event in 10 models (BCM02 data not included), in reanalyses of the National Center for Environmental Prediction (NCEP, http://www.cdc.noaa.gov/cdc/reanalysis/reanalysis.shtml) and the European Centre for Medium-range Weather Forecasts (ECMWF, http://www.ecmwf.int/research/era/ERA-15/), as well as in the HadISST 1.1 sea surface temperature dataset (http://badc.nerc.ac.uk/data/hadisst/). The shaded area represents the one-standard-deviation envelope of the observed NIÑO3 sea surface temperature anomaly for warm events in the HadISST 1.1 dataset. In Figure 3b the maximum entropy power spectra calculated from the available CMIP2+ model monthly mean surface air temperature anomalies are compared with that obtained from HadISST1.1 sea surface temperature anomalies, both for the NIÑO3 region (BCM02 model data not included). Vertical lines correspond to 2- and 7-year periods, respectively.

Figure 1

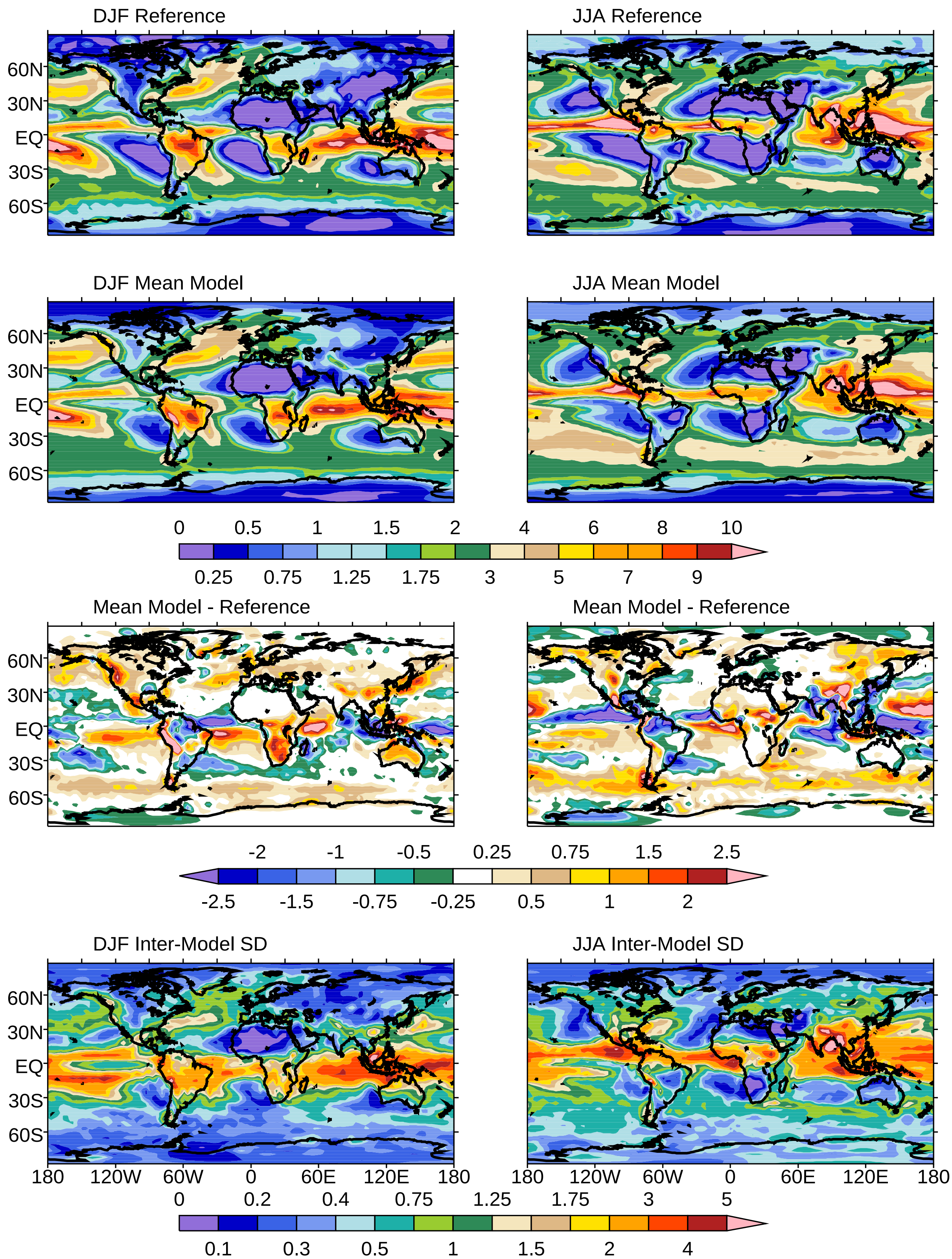
DJF Reference
JJA Reference
DJF Mean Model
JJA Mean Model
0 0.5 1 1.5 2 4 6 8 10
0.25 0.75 1.25 1.75 3 5 7 9
Mean Model - Reference
Mean Model - Reference
-2 -1 -0.5 0.25 0.75 1.5 2.5
-2.5 -1.5 -0.75 -0.25 0.5 1 2
DJF Inter-Model SD
JJA Inter-Model SD
60N 30N EQ 30S 60S
180 120W 60W 0 60E 120E 180
0 0.2 0.4 0.75 1.25 1.75 3 5
0.1 0.3 0.5 1 1.5 2 4

Figure 2

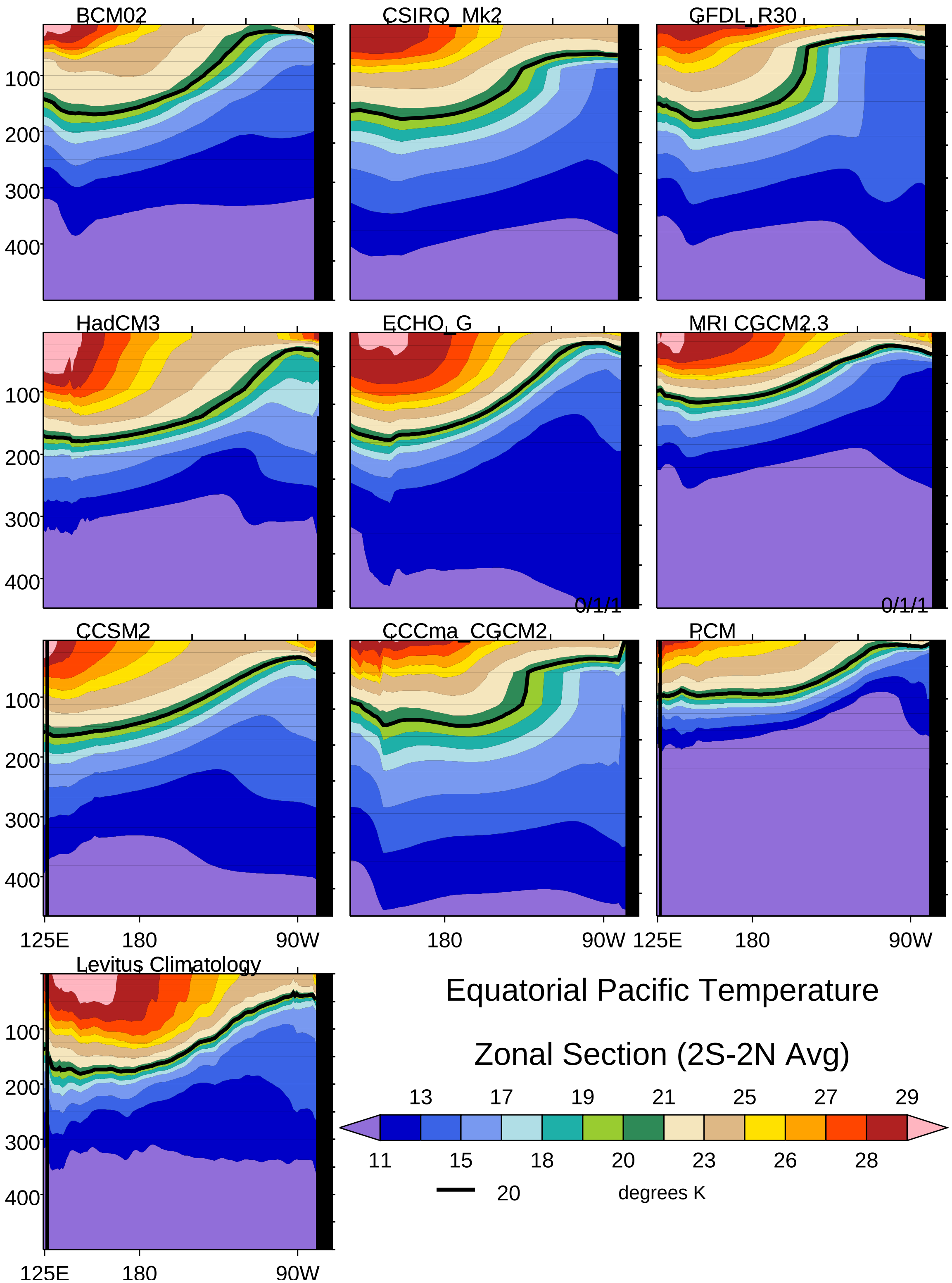
BCM02
CSIRO_Mk2
GFDL_R30
HadCM3
ECHO_G
MRI CGCM2.3
CCSM2
CCCma_CGCM2
PCM
Levitus Climatology
100
200
300
400
0/1/1
0/1/1
125E
180
90W
Equatorial Pacific Temperature
Zonal Section (2S-2N Avg)
13
17
19
21
25
27
29
11
15
18
20
23
26
28
20
degrees K

Figure 3a

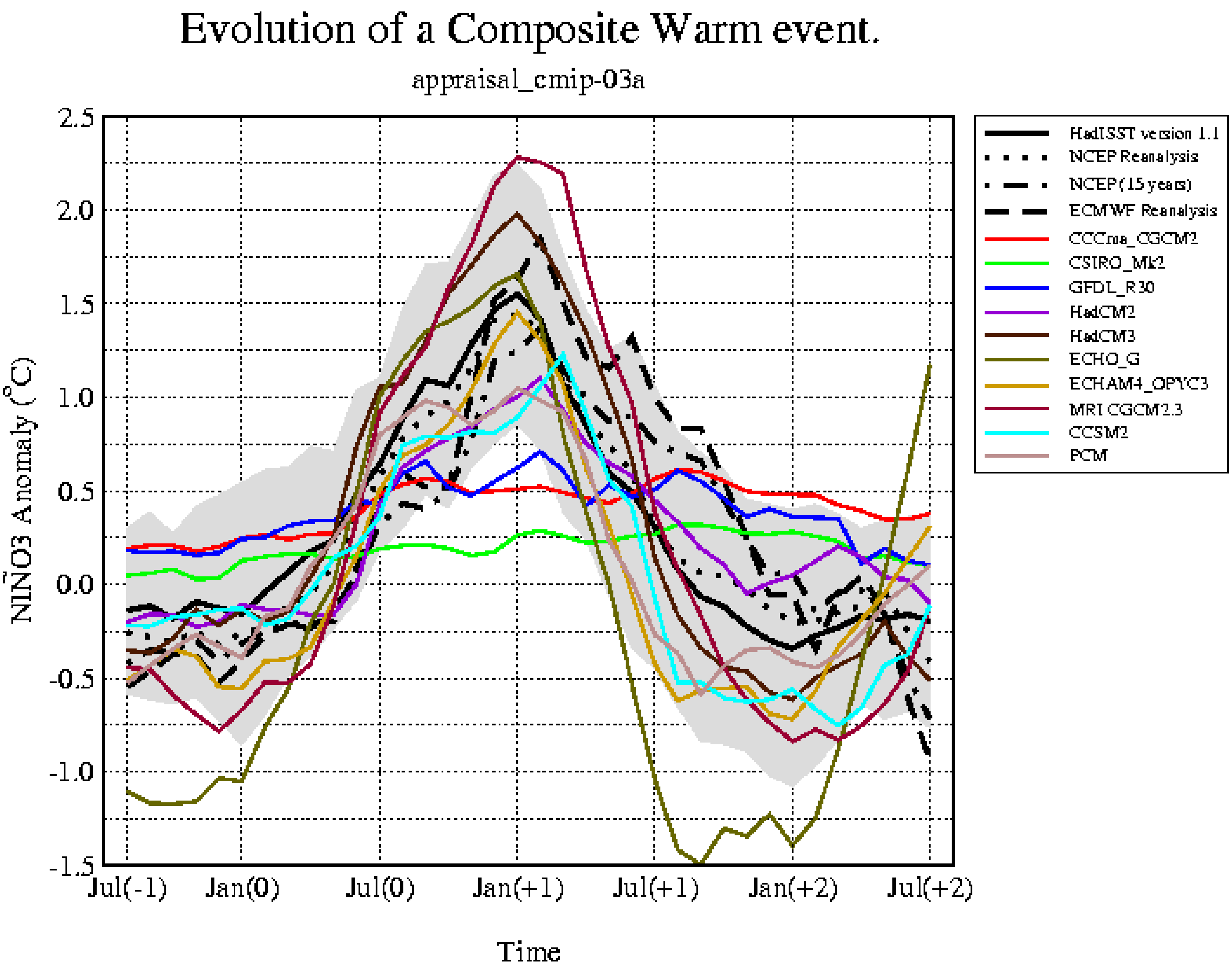

Evolution of a Composite Warm event.
appraisal_cmip-03a
NIÑO3 Anomaly (°C)
2.5
2.0
1.5
1.0
0.5
0.0
-0.5
-1.0
-1.5
Jul(-1)
Jan(0)
Jul(0)
Jan(+1)
Jul(+1)
Jan(+2)
Jul(+2)
Time
HadISST version 1.1
NCEP Reanalysis
NCEP (15 years)
ECMWF Reanalysis
CCCma_CGCM2
CSIRO_Mk2
GFDL_R30
HadCM2
HadCM3
ECHO_G
ECHAM4_OPYC3
MRI CGCM2.3
CCSM2
PCM

Figure 3b

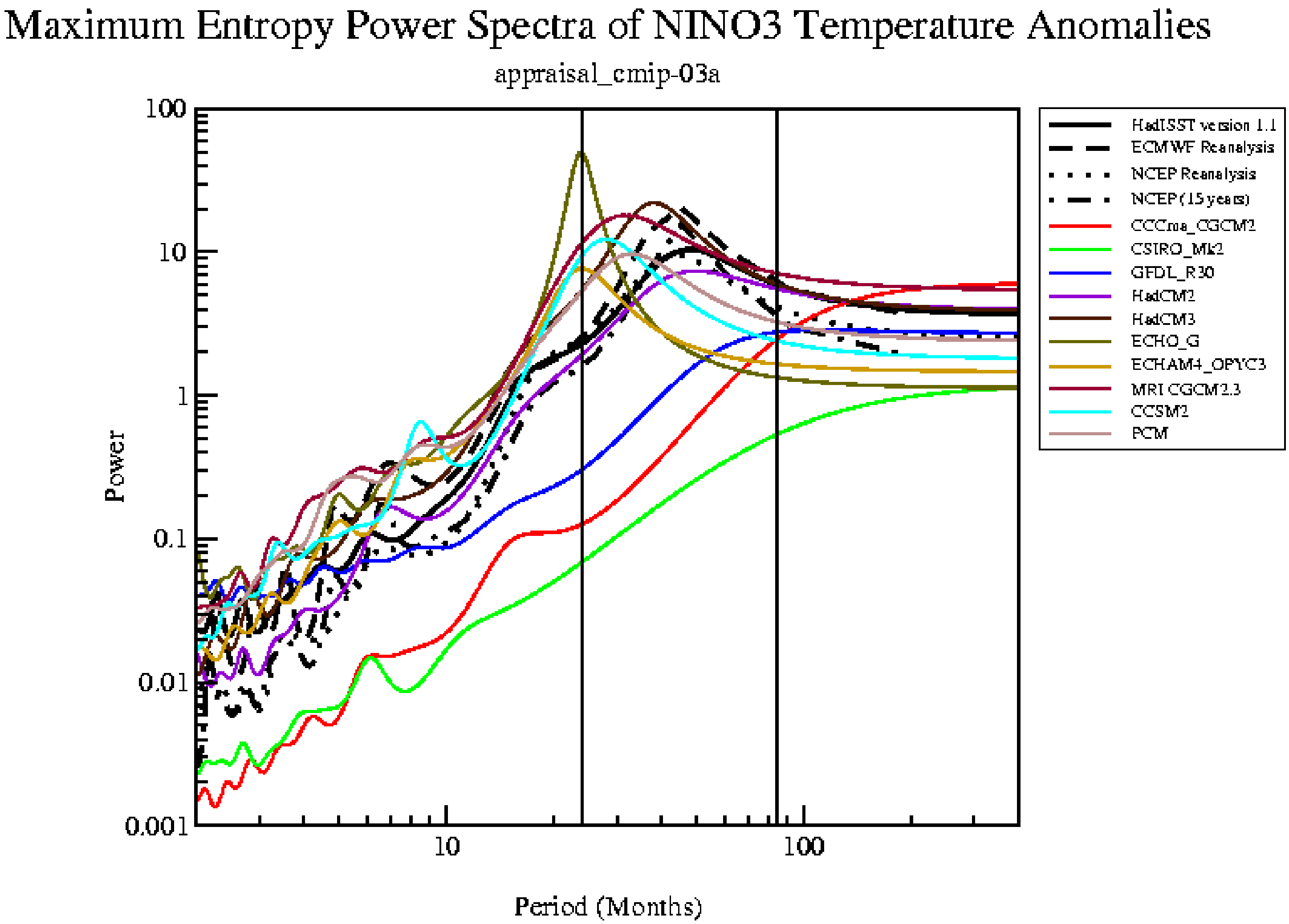
Maximum Entropy Power Spectra of NINO3 Temperature Anomalies
appraisal_cmip-03a
Power
Period (Months)
100
10
1
0.1
0.01
0.001
10
100
HadISST version 1.1
ECMWF Reanalysis
NCEP Reanalysis
NCEP (15 years)
CCCma_CGCM2
CSIRO_Mk2
GFDL_R30
HadCM2
HadCM3
ECHO_G
ECHAM4_OPYC3
MRI CGCM2.3
CCSM2
PCM